NASA Technical Memorandum 89410

Vortex Breakdown and Control Experiments in the Ames-Dryden Water Tunnel

F.K. Owen and D.J. Peake

November 1986

NASA

National Aeronautics and
Space Administration

Vortex Breakdown and Control Experiments in the Ames-Dryden Water Tunnel

F. K. Owen,
D. J. Peake, Ames Research Center, Moffett Field, California

November 1986

NASA

National Aeronautics and
Space Administration

Ames Research Center
Moffett Field, California 94035

VORTEX BREAKDOWN AND CONTROL EXPERIMENTS IN THE AMES-DRYDEN WATER TUNNEL

F. K. Owen
Complere, Inc.
P. O. Box 1697
Palo Alto, California 94302

and

D. J. Peake
NASA Ames Research Center
Moffett Field, California 94035

SUMMARY

Flow-field measurements have been made to determine the effects of core blowing on vortex breakdown and control. The results of these proof-of-concept experiments clearly demonstrate the usefulness of water tunnels as test platforms for advanced flow-field simulation and measurement.

1. INTRODUCTION

At present, there are significant efforts being made to effect design changes which will improve aircraft agility, maneuverability, and performance. But although significant progress has been made in computational aerodynamics, reliable design changes still cannot be made without recourse to experiment. Attempts to extend tactical flight envelopes require extensive, preflight, ground-based model testing. Unfortunately, conventional wind tunnel testing is expensive and time consuming and most facilities were built before present-day optical methods for quantitative flow field measurements were envisaged. Consequently, there are few nonintrusive, detailed measurements of lee-side vortex flow fields, which are often required to support design evaluation and optimization.

However, in the past, qualitative water tunnel simulations have guided many practical designs and, since most of these facilities have been built with excellent optical access, they are ideally suited for use in advanced flow-field diagnostics. Since the performance of most lifting and maneuvering bodies is governed by extensive viscous wakes and vortical lee-side flows, nonintrusive optical measurement techniques are required. Consequently, water tunnels offer the opportunity to obtain inexpensive, detailed,

flow-field measurements to support "cut and try" designs and basic research. Water tunnels are excellent media for conventional and scanning laser velocimetry research (Ref. 1) and laser fluorescence anemometer studies of mixing processes (Ref. 2).

This paper describes an experiment in which detailed qualitative and quantitative flow-field observations of vortex breakdown were obtained and describes some of the results of attempts to control its occurrence. Specifically, the experiment was designed to determine the mechanisms and feasibility of controlling vortex breakdown by introducing relatively low rates of jet blowing along the vortex core.

2. BACKGROUND

When a slender delta wing is at an angle of attack to an oncoming stream, the upper- and lower-surface boundary layers flow outward and separate from the leading edges to form two free shear layers that roll up into a pair of vortices above the wing. Increasing angle of attack strengthens the vortices until the induced wing pressure field and associated adverse streamwise pressure gradients cause vortex breakdown. The flow is further complicated as the leading-edge vortices mix with the wake from the trailing edge downstream of the wing. The phenomenon of vortex breakdown (or vortex bursting) can have a significant influence on control-surface performance and unsteady loading. The inherent unsteadiness of the breakdown process compounds the problem as it continually moves the breakdown region back and forth along the vortex axis. This creates serious time-dependent flow problems and asymmetrically disposed breakdown positions above the wing that are aggravated with sideslip.

Wide variations of breakdown patterns have been observed. With increasing swirl, the patterns change from spiral to near axisymmetric (Ref. 3). Spiral breakdown most commonly occurs over delta wings. In this breakdown process, the filament of fluid along the axis does not spread out symmetrically from a fixed stagnation point but, instead, takes on a spiral form around an unsteady "stagnation point" which varies in both space and time. Axisymmetric breakdown over delta wings, although rare, can also occur (Ref. 4). In this case, the vortex has a roughly axisymmetric breakdown pattern with a characteristic bubble, which can have single or multiple tails (Ref. 5).

Unfortunately, the parameters and conditions that result in vortex breakdown are poorly understood because reliable quantitative experimental data are difficult to obtain. With limited experimental information to guide flow-field modeling, numerical studies of vortex breakdown and control have met with only limited success (Ref. 6). There have been two principal reasons for this. First, flow-field unsteadiness associated with breakdown produces directional intermittency. This leads to large uncertainties in mean and unsteady flow measurements obtained with conventional pitot and hot-wire probes. Second, and perhaps

more important, is the fact that vortex breakdown is known to be extremely sensitive to any form of intro-
duced disturbance. Probes, because of their blockage, may drastically alter the breakdown position. For
these reasons, almost complete reliance has been placed on flow-visualization techniques to determine
flow-field characteristics. But, with the advent of the laser velocimeter, there are now opportunities to
determine accurate, quantitative, flow-field velocity measurements of the vortex bursting process.

3. EXPERIMENTAL DETAILS

The experiment discussed here was conducted in the NASA Ames-Dryden Water Tunnel. A general layout
of this closed-return facility which has a 41- by 61-cm vertical test section is shown in Fig. 1. The
four walls are made of plexiglass, which provides excellent optical access for both flow visualization and
laser velocimetry. The tunnel is driven by a 50-hp ac motor and the volume flow rate is controlled by a
butterfly valve to produce test section flow velocities of up to 35 cm/sec. The flow quality is con-
trolled by three honeycombs in the tunnel circuit, one of which is located at the test section entry after
an effective contraction ratio of 5:1 (Fig. 1).

The test configuration which consisted of a 45° half delta planform model upstream of a 16-mesh
screen is shown in Fig. 2. The tests were conducted at a free-stream velocity of 11 cm/sec and a model
angle of attack of 15°. The purpose of the screen was to produce an adverse pressure gradient sufficient
to cause vortex breakdown in the test section ahead of the screen. To control vortex bursting, a small
blowing tube was installed at the apex of the half-delta wing through which jets, at velocities higher
than the free stream, could be pumped along the core of the tip vortex. The blowing system provided for a
maximum jet-momentum coefficient, based on wing planform area, of 0.14 at the maximum jet blowing
pressure.

In the past, air or hydrogen bubbles have been used as tracers to visualize flow patterns in water
tunnels. For steady flows, streak lines can be identified with streamline patterns. However, in more
complex flows of practical interest, the use of bubbles for flow visualization has distinct drawbacks.
First of all, their introduction acts as a fluid lubricant which alters the apparent fluid viscosity and
therefore its turbulent structure. Second, light refraction at the gas/water interfaces will destroy
laser beam coherence and make it impossible to obtain laser velocimeter measurements in the regions where
the tracer is present. In the current experiment, the vortex flow field was visualized by injecting
fluorescent dyes of different colors through the vortex control tube and from a port near the apex of the
model. Horizontal and vertical laser light sheets were generated using an argon-ion laser and a series of
cylindrical lenses which produced a variable, thin sheet of laser light that could be focused at different
planes in the flow field. The horizontal fluorescent sheets showed flow features in the cross-flow plane,
whereas the vertical sheets showed the streamwise flow development. Axial and radial flow visualization
scans were recorded on video tape.

Three component laser velocimeter measurements were made with the system shown in Fig. 3. This
fringe mode, forward scatter system, which utilized the 4880- and 5145-Å lines of an argon-ion laser, was
specifically designed to measure all three components of the vortex velocities by measuring the flow with
two different traverse configurations. The computer-controlled traverse system was configured such that
successive orthogonal scans measured the axial and tangential (swirl) components and the axial and radial
velocities, respectively. Bragg-cell frequency-shifting, which is required for probing directionally
intermittent flow fields, was incorporated in both spectral lines. Two traversing systems are shown. The
one on the opposite side of the test section from the laser holds the collecting lens and photodetectors
for forward-scatter light collection. The traversing system on the laser side of the test section sup-
ports the transmitting lenses. Mirrors fixed to this traversing system permit three-dimensional scanning
of the velocimeter's sensing volume; the other optics remain stationary. Both traversing systems are
driven with computer-controlled stepper motors.

Naturally occurring particles in the tunnel flow were used for light scattering. No additional seed-
ing was required. Single-particle signal processing was used to determine local time-dependent veloc-
ities. From these determinations, the local time-averaged velocities and velocity fluctuation levels were
calculated. Fluctuating velocity cross-correlations were also obtained by requiring co-incidence on each
pair of instantaneous velocity occurrences. On-line data acquisition and display were achieved by means
of desk-top computer analysis. Details are given in Ref. 7. Prudent selection of data-acquisition elec-
tronics and optical components enabled us to achieve velocity sensitivities down to 1 mm/sec, which were
adequate for the present investigation.

4. TEST RESULTS

4.1 Laser Vapor Screen

In the absence of jet blowing, vortex breakdown was clearly visible ahead of the mesh screen. Large-
scale, unsteady motions associated with directional intermittency throughout the vortex core were appar-
ent. These motions were associated with time-dependent axial changes in vortex breakdown position.
Closer visual inspection showed that the breakdown was of a spiral type, which is the form most commonly
observed in the flow over delta wings at high angle of attack. At breakdown, the dye filament marking the
spiral axis decelerated to form an abrupt kink. But the filaments did not spread out initially. Instead,
they took the form of a spiral that persisted for several turns before breaking up into large-scale

2

turbulent-like flow. These time-dependent spiraling occurrences appeared to move randomly in the cross-flow plane and along the vortex axis.

The effects of jet blowing can be divided into stabilizing and destabilizing regimes that are dependent on the jet excess velocity relative to the free stream. At low blowing rates, the time-dependent spiraling movement along the axis is suppressed, although breakdown still occurs and cross-flow visualization shows that there is still signficant large-scale turbulent-like mixing and movement of the vortex core prior to breakdown. As the jet intensity is increased, the flow in both the longitudinal and cross-flow planes is continually stabilized until at an optimum jet momentum coefficient of 0.05, for these experiments, bursting is completely suppressed and vortex trajectory meandering is stabilized. Further increases in jet velocity tend to increase lateral growth and motion. There is, then, a general increase in flow-field large-scale unsteadiness although vortex bursting continues to be suppressed. Examples of cross-flow, laser-light-sheet-fluorescence flow visualization are shown in Fig. 4.

4.2 Flow-Field Measurements

Based on the visual observations, three axial stations were chosen for extensive mean and unsteady flow documentation. These stations covered the initial and developing jet interaction, and the spiraling and breakdown regions. Tunnel centerline velocity measurements were also made with the model removed to determine the flow-field adverse pressure gradient caused by the screen. These results, shown in Fig. 5, provide a necessary boundary condition for any future flow-field computations.

The mean axial and tangential velocity profiles measured three and four chords from the model apex are shown in Figs. 6 and 7. The "no blowing" axial velocity profiles show that there is a progressive decrease in vortex core momentum as breakdown approaches. Comparisons of the no-blowing axial profiles at $x/c = 3.0$ and 4.0 show not only a general deceleration of the mean flow as the time-dependent breakdown region is approached, but also a much wider spanwise deficit at the $x/c = 4.0$ station because of accentuated meandering of the vortex spiral. Clearly, axial blowing along the core can overcome and reverse this momentum deficit for a substantial distance downstream. This effect is shown in more detail over the entire jet-blowing pressure range in Fig. 8.

The swirl profiles show that initially each vortex has an outer free vortex form with an inner viscous core. The swirl number of 0.3, based on the ratio of the measured maximum local tangential and free-stream velocities is indicative of "moderate" vortex strength. The principal feature of each set of tangential velocity profiles is the progressive downstream decrease in the maximum induced velocity and mean gradient across the core. A comparison of these tangential and axial velocity profiles shows that the momentum addition due to blowing enhances the core of the swirling flow in such a way that deceleration of both axial and tangential velocity components is alleviated near the axis. As a result, vortex strength is increased and breakdown is delayed. Radial velocity profiles, Fig. 9, show that there are also significant increases due to core meandering associated with vortex breakdown. It is also an indication of increased time-dependent flow angularity in the cross-flow plane.

Detailed analysis of the test results shows that there is an optimum blowing rate for vortex stabilization and control. Consider first the comparison of the tangential velocity profiles shown in Fig. 10. Clearly, the highest jet-blowing pressure degrades the vortex, reducing both the maximum induced tangential velocity and the mean gradient across the viscous core. Comparisons of this type have been used to determine the increases in maximum tangential velocity and vorticty induced by jet blowing. Figure 11 shows the effect of jet blowing on the measured maximum induced tangential velocity normalized by the value observed without blowing. The effect is clearly significant, especially at the $x/c = 4.0$ station. An indication of the vorticity induced by jet blowing is given in Fig. 12, where it can be seen that vorticity levels of up to three times the baseline value can be achieved at the optimum jet-velocity ratio. At higher blowing pressures, significant reductions occur, and even detrimental results are apparent at the highest blowing rates. Calculated vorticity decay rates shown in Fig. 13 confirm the favorable effects of moderate axial blowing, which can double the extent of axial vortex preservation. Figure 14 shows that, with optimum blowing, the axial vorticity transport can be increased by almost an order of magnitude.

Some insight into the unsteady features of vortex breakdown can be determined from the fluctuating flow measurements. The axial velocity disturbance levels, measured along the core, Fig. 15, show that, although some flow reversal is still present at the lower velocities, jet blowing produces a dramatic improvement in vortex stability followed by some slight degradation at high jet velocities. Dramatic disturbance-level reductions across the entire vortex core can be achieved with optimum jet blowing (Fig. 16). Since local unsteadiness levels above 30% indicate points in the flow at which instantaneous flow reversal occurs, we can see that, without jet blowing, there is a significant region of directionally intermittent flow. This region is completely removed with blowing. There is a significant stabilization of the flow field as vortex breakdown no longer occurs and local ratios of the dynamic loadings are reduced by factors of up to 20. Tangential centerline turbulent-like mixing-length scales have also been calculated using the local disturbance levels and mean flow gradients. These results, Fig. 17, show that, without blowing, the mixing-length scales, which are related to vortex movement in the cross-flow plane, are about equal to the extent of the local time-averaged viscous core. Optimum blowing reduces these scales by almost a factor of three, although the detrimental effects of excess jet blowing are more clearly evident. Centerline axial mixing-length scales based on measured axial velocity fluctuation levels and mean axial velocity gradient are significantly larger. They indicate that, without jet blowing, the extent of the breakdown region is comparable to that of the model chord length.

3

Turbulence modeling of these flows will also require an understanding of the mixing mechanisms between a free jet issuing into a surrounding swirling flow field. Figure 18 compares the free-jet velocity profile with that measured within the vortex. It is apparent, from the differences in spreading rate, that there are significant changes in the entrainment and mixing mechanisms in the two cases. Apparently there is some centrifugal-force stabilization of the large-scale mixing and entrainment mechanisms. The effect of swirl is to restrict the jet entrainment and confine its influence along the core. This confinement improves jet effectiveness in providing an effective sink which preserves vortex coherence, lifetime, and stability. Additional insight into the turbulent-like nature of the vortex flow fields, with and without jet blowing, can be deduced from Figs. 19 and 20, which show the correlation between the large-scale axial and tangential fluctuations. Comparisons of the results at the x/c = 3.0 and 4.0 stations clearly show the spanwise increase in vortex meandering as breakdown occurs in the zero jet-flow velocity case. This wandering generates an extensive region of high levels of apparent shear stress that can be significantly confined and stabilized with blowing.

5. CONCLUDING REMARKS

The results of this simple experiment show that vortex breakdown can be controlled, and eliminated, by relatively small amounts of jet blowing along the vortex axis. For this particular experiment, an optimum value of jet-momentum coefficient for vortex control has been identified. This optimum value of 0.05 corresponds to a jet excess momentum equal to the vortex-core-momentum deficit without blowing. In restrospect, it is not too surprising that the most efficient jet-blowing pressure minimized the axial mean-velocity gradients across the vortex. In simplistic terms, this means that the jet gave the wing vortex an initial "push," which moved it with the local mean velocity; therefore, in the Lagrangian frame it was "unaware" of convection. Consequently, minimal energy was extracted from the vortex by mean-axial-velocity gradients.

Of course, optimum blowing conditions may well be different in other, more practical situations. However, this optimization criterion may still hold and the experimental approach investigated here could well prove effective if it is applied to leading-edge-extension (LEX) vortex control of twin-tail fighter aircraft. Successful application could lead to significant reductions in time-dependent dynamic loading and flow angularity associated with vortex breakdown. Vortex control could greatly alleviate structural fatigue and improve control-surface effectiveness and response.

Finally, this work clearly demonstrates how water tunnels can be used in conjunction with advanced optical techniques to provide nonintrusive, detailed, flow-field measurements of complex fluid flows with a minimum of expense.

REFERENCES

1. Owen, F. K., "A Scanning Laser Velocimenter for Turbulence Research," NASA CR-172493, 1984.

2. Owen, F. K., "Measurements of Instantaneous Velocity and Concentration in Turbulent Mixing Flows," AGARD CPP-193, 1976.

3. Sarpkaya, T., "Vortex Breakdown in Swirling Conical Flows," AIAA J., Vol. 9, No. 9, 1971, p. 1792.

4. Lambourne, N. C. and Bryer, D. W., "The Bursting of Leading Edge Vortices--Some Observations and Discussion of the Phenomenon," Brit. A.R.C.R. & M., No. 3282, 1962.

5. Faler, J. H. and Leibovich, S., "Disrupted States of Vortex Flow and Vortex Breakdown. Phys. Fluids, Vol. 20, No. 9, 1977, p. 1385.

6. Karashima, K. and Kitama, S., "The Effect of a Small Blowing on Vortex-Breakdown of a Swirling Flow," Computational Techniques & Applications: CTAC-83, 1984, p. 553.

7. Owen, F. K., Orngard, G. M. and McDevitt, T. K., "A New 3D LDV System for the NASA Ames 6 × 6 ft. Wind Tunnel," IEEE, 85-CH-2210-3, 1985, p. 257.
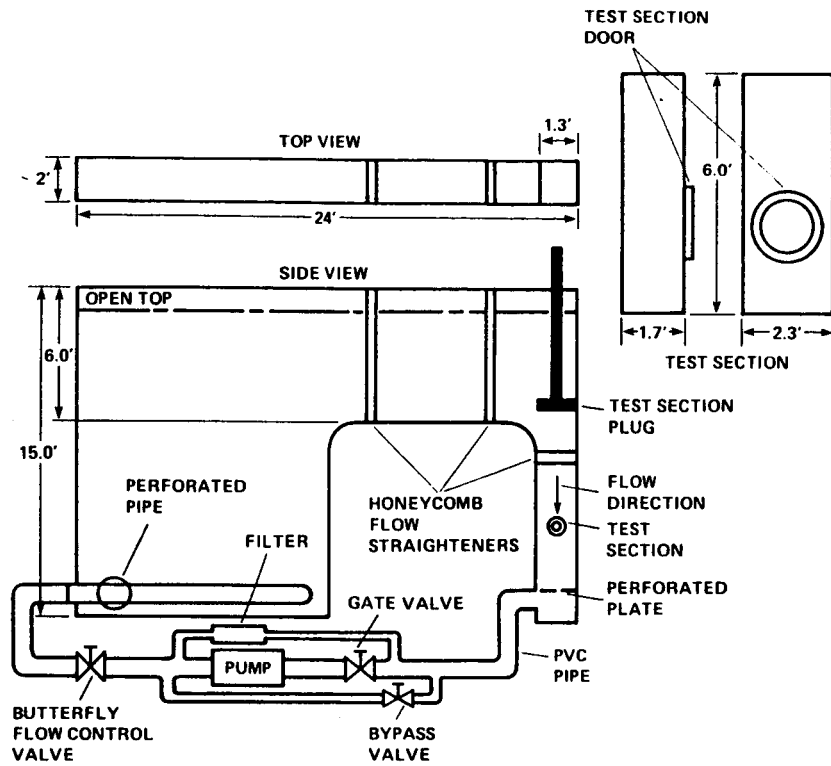
TOP VIEW

SIDE VIEW

TEST SECTION

Figure 1. Layout of NASA Ames-Dryden water tunnel.
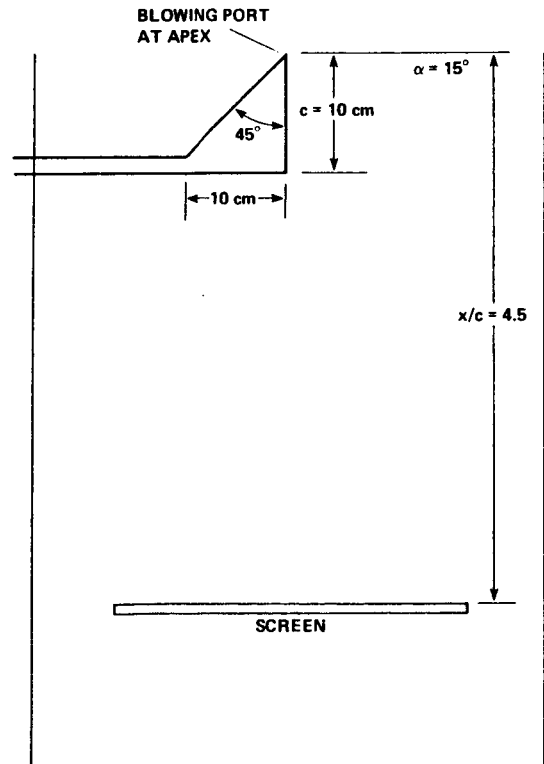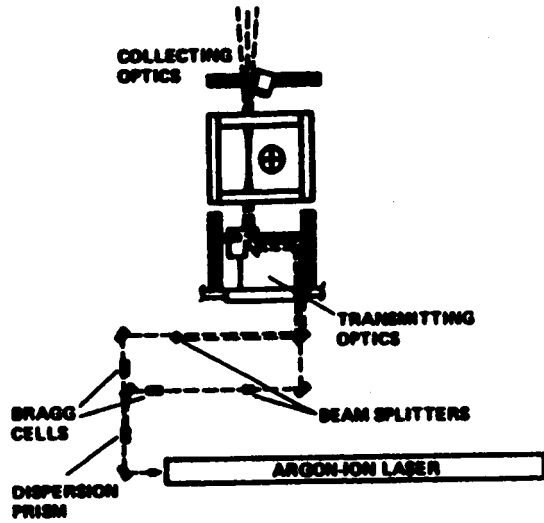

Figure 2. Water tunnel test aparatus.

Figure 3. Laser velocimeter.

$C\mu = 0$

$C\mu = 0.05$

$C\mu = 0.10$

Figure 4. Laser fluorescence light sheets
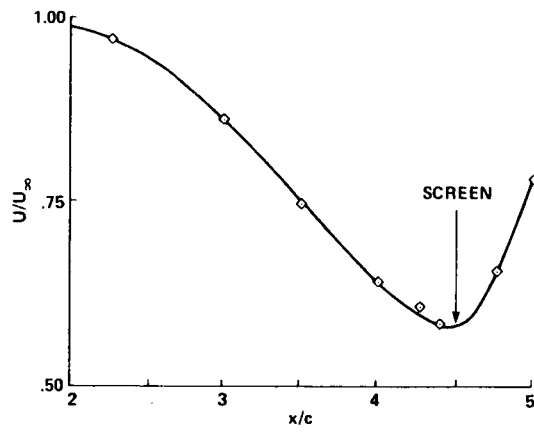illuminating the cross-flow plane, x/c = 4.0.

6

Figure 5. Axial velocity profile along the centerline of the
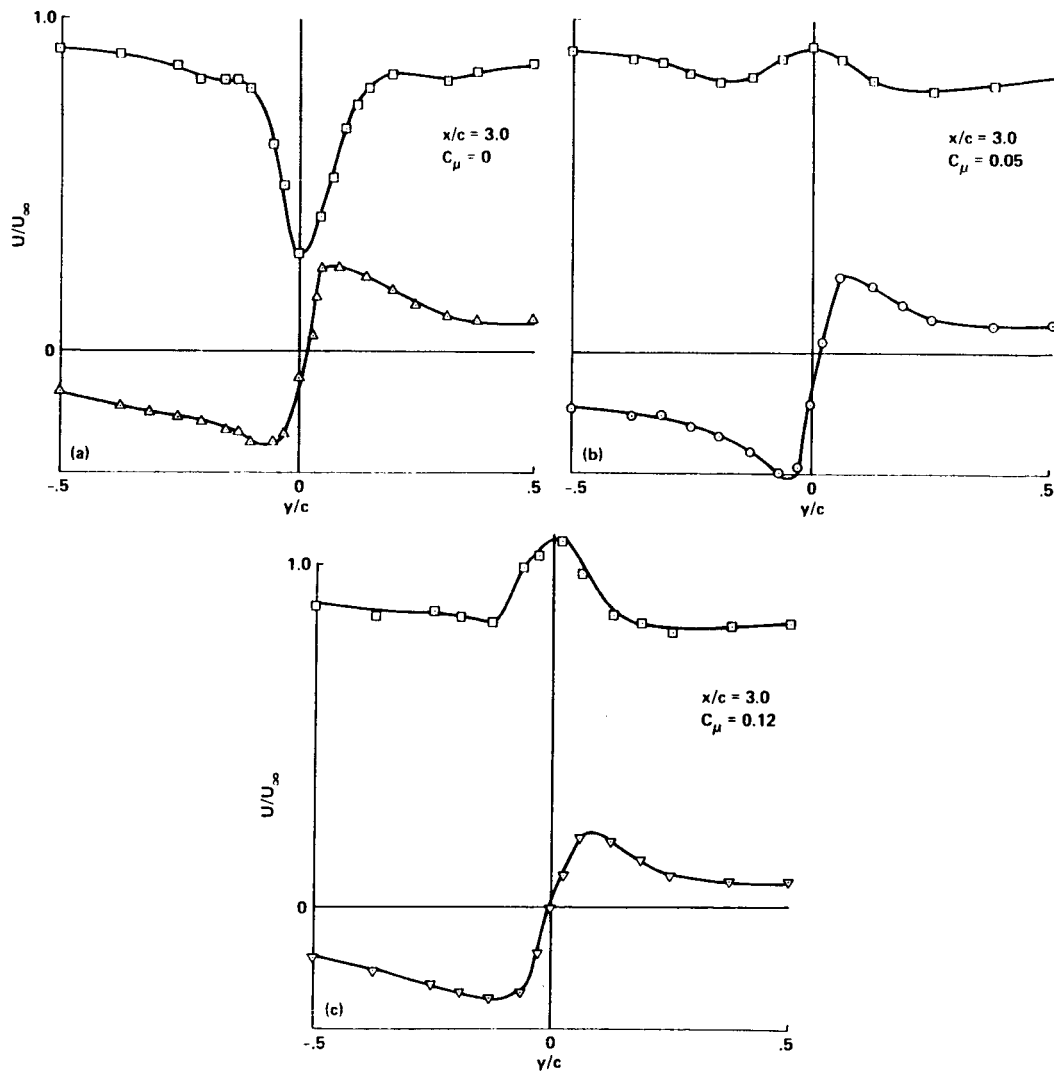test section with the screen installed.

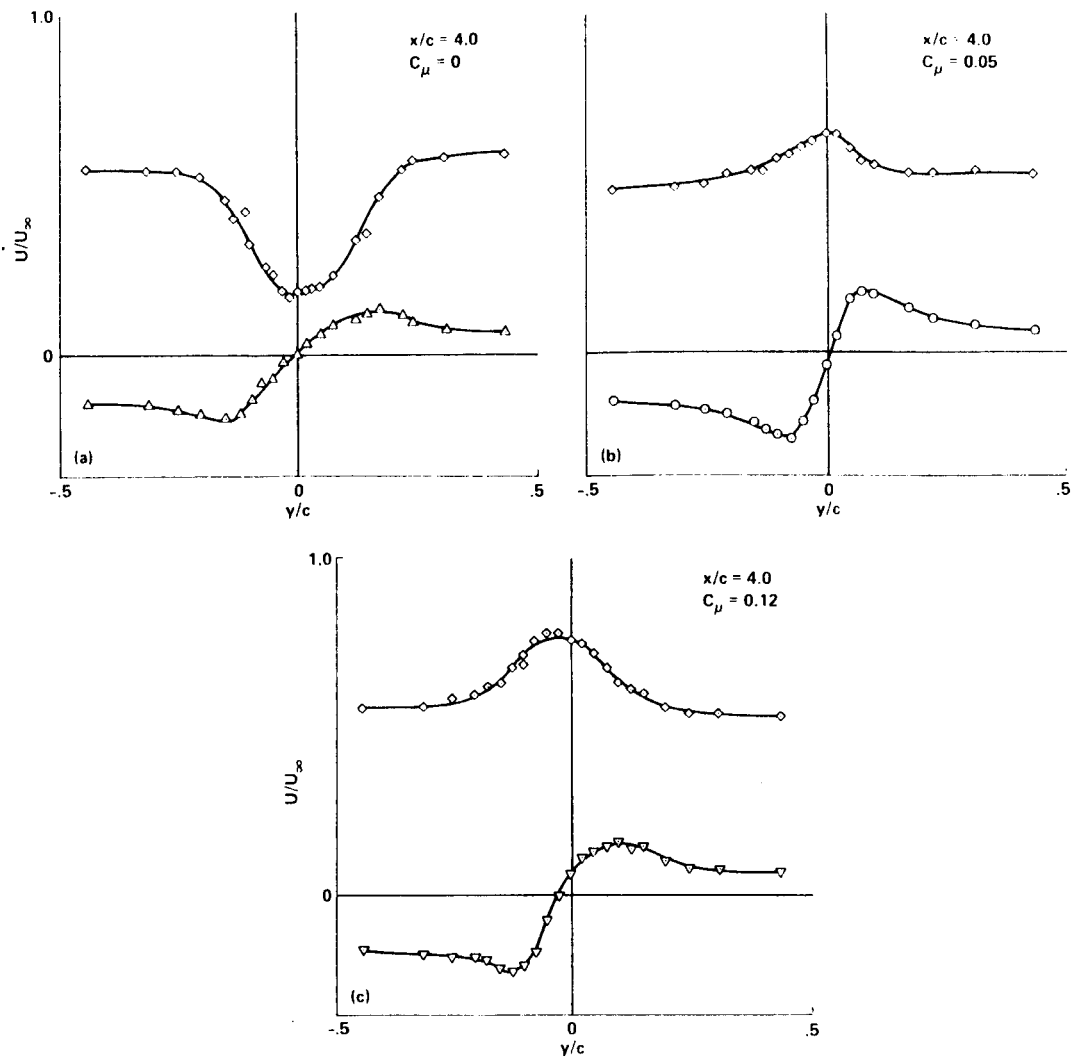Figure 6. Time-averaged axial and tangential velocity profiles, x/c = 3.0.

7

Figure 7. Time-averaged axial and tangential velocity profiles, x/c = 4.0.
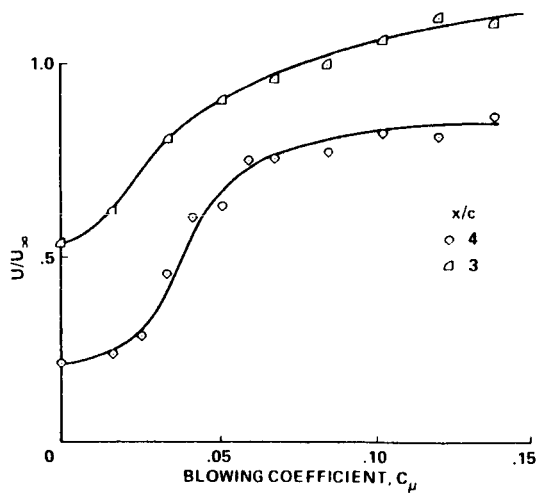
Figure 8. Influence of jet blowing on vortex-core axial velocity profiles.
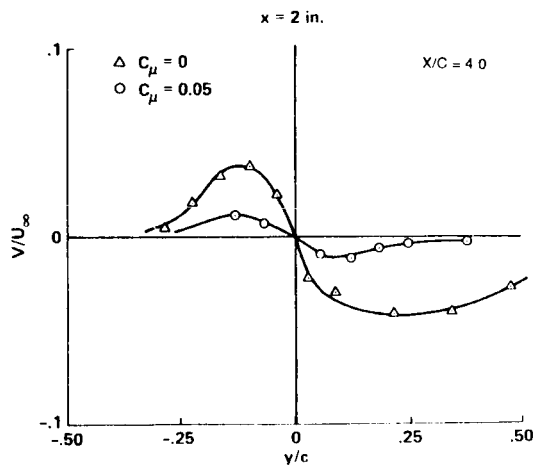
Figure 9. Influence of jet blowing on radial velocity profiles.
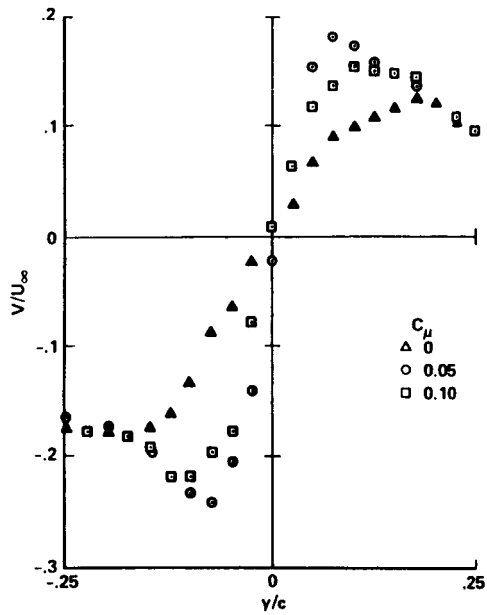
Figure 10. Comparison of tangential velocity profiles, x/c = 4.0.
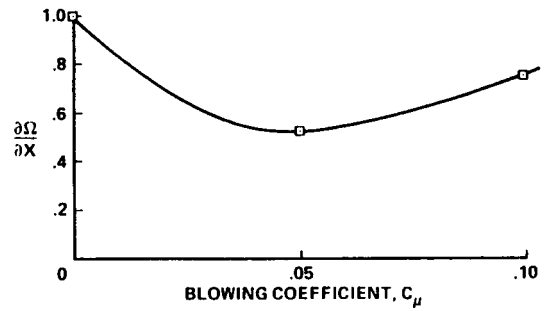
Figure 13. Streamwise vorticity decay rates.
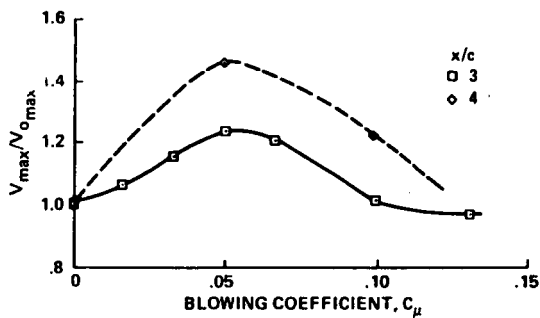
Figure 11. Tangential velocity induced by blowing.
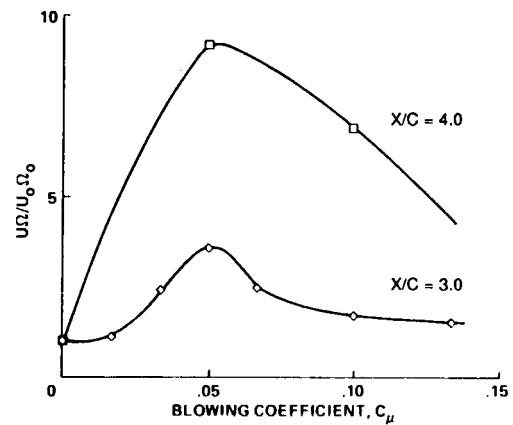
Figure 14. Steamwise vorticity convection rates.
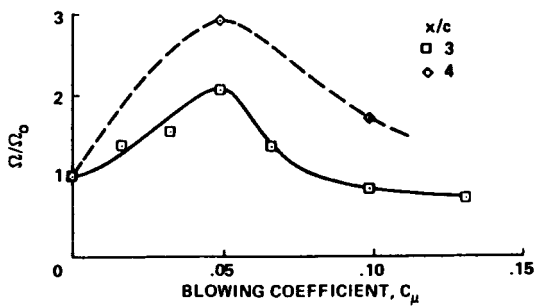
Figure 12. Streamwise vorticity induced by blowing.
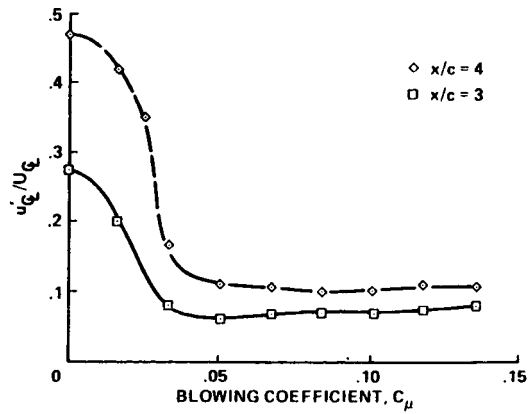
Figure 15. Influence of jet blowing on axial velocity fluctuation levels.

9
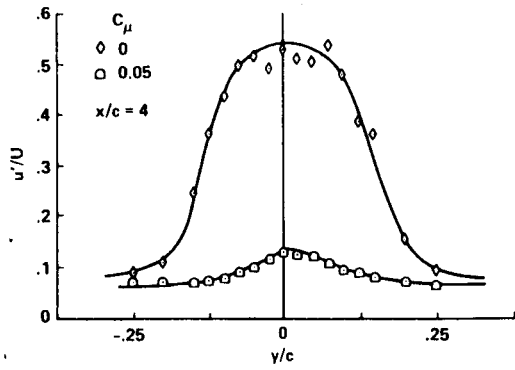
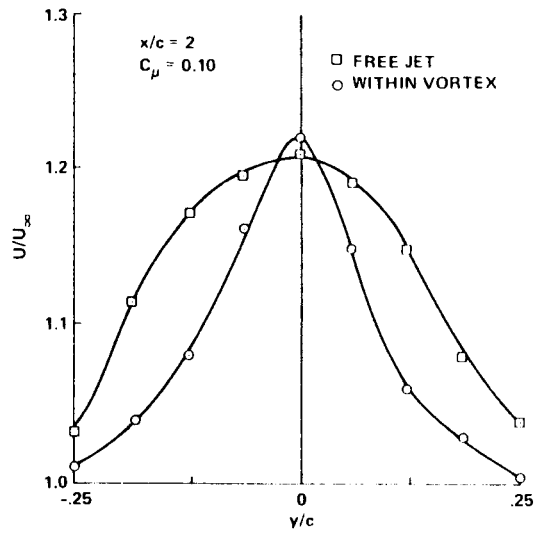Figure 16. Influence of jet blowing on local
axial fluctuation levels.

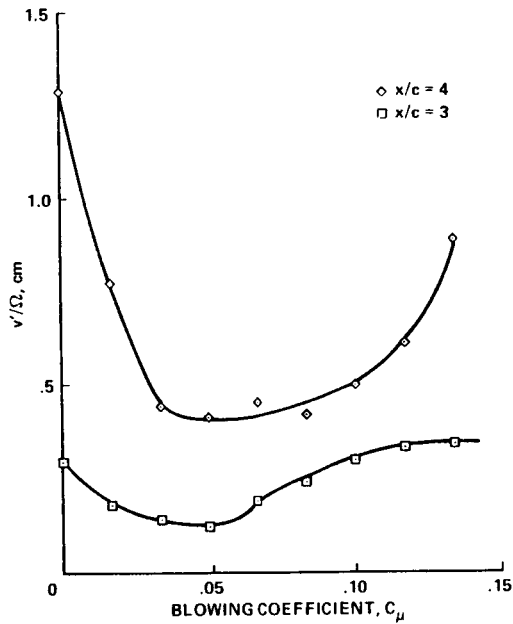Figure 18. Free- and confined-jet flow profiles.

Figure 17. Influence of jet blowing on tangen-
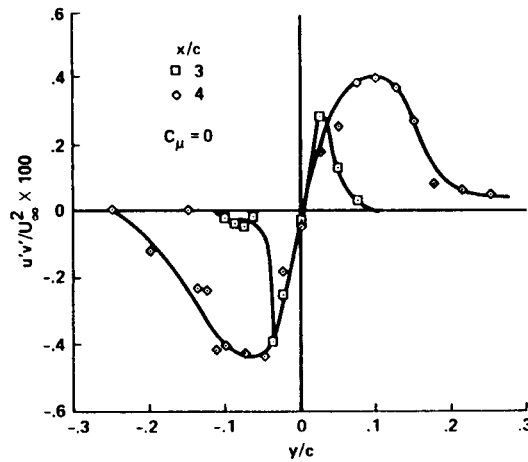tial velocity fluctuating length scales.

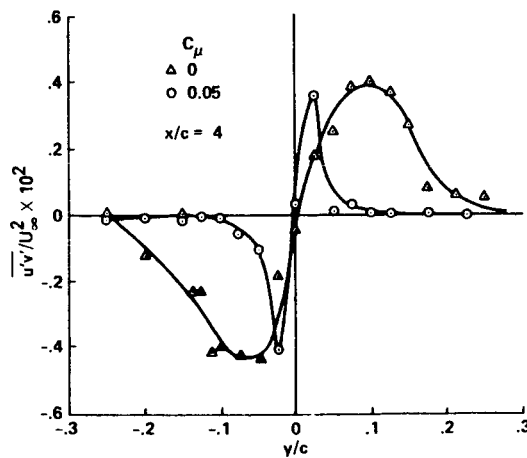Figure 19. Axial variation of fluctuating
velocity cross correlations.

Figure 20. Influence of blowing on the fluc-
tuating velocity cross correlations.

10

1. Report No. NASA TM-89410	2. Government Accession No.	3. Recipient's Catalog No.
4. Title and Subtitle VORTEX BREAKDOWN AND CONTROL EXPERIMENTS IN THE AMES-DRYDEN WATER TUNNEL		5. Report Date November 1986
		6. Performing Organization Code
7. Author(s) F. K. Owen (Complere, Inc., P. O. Box 1697, Palo Alto, CA 94302) and David J. Peake		8. Performing Organization Report No. A-87030
9. Performing Organization Name and Address Ames Research Center Moffett Field, CA 94035		10. Work Unit No.
		11. Contract or Grant No.
12. Sponsoring Agency Name and Address National Aeronautics and Space Administration Washington, DC 20546		13. Type of Report and Period Covered Technical Memorandum
		14. Sponsoring Agency Code 505-61-71

16. Abstract

Flow-field measurements have been made to determine the effects of core blowing on vortex breakdown and control. The results of these proof-of-concept experiments clearly demonstrate the usefulness of water tunnels as test platforms for advanced flow-field simulation and measurement.

17. Key Words (Suggested by Author(s)) Aircraft aerodynamics Vortex flow control Laser anemometry	18. Distribution Statement Unclassified-Unlimited Subject Category - 02
19. Security Classif. (of this report) Unclassified	20. Security Classif. (of this page) Unclassified	21. No. of Pages 11	22. Price* A01